2018 European Control Conference (ECC)
June 12-15, 2018. Limassol, Cyprus

Human Motion Prediction in Human-Robot Handovers based on Dynamic Movement Primitives

Dominik Widmann[1] and Yiannis Karayiannidis[1,2]

Abstract— **Human-robot handovers can be made more seamless by predicting handover place and time on-line as soon as the human agent initiates a handover process. We consider the prediction problem as a model-based parameter estimation problem where the point attractor and the timescale of human hand motion are estimated on-line. Using dynamic movement primitives as a parameterization of human motion, its point attractor and timescale are successfully estimated on-line using an extended Kalman filter. Convergence of the parameter estimates is shown and the performance of the proposed predictor is evaluated using generated trajectories as well as experimental data of human-human handovers. Thanks to the good prediction of the handover place, the presented algorithm can be used to improve human-robot collaboration.**

I. Introduction

In recent years, robots have come to provide an essential contribution to productivity in industrial settings. Usually, humans and robots working in production are separated by cages, leading to almost no collaboration between the two. Recent advancements on robotic technologies, however, foresee a strong collaboration between humans and robots in the near future. Higher efficiency in both industrial and domestic tasks is expected for humans and robots that work together. According to the Strategic Research Agenda for Robotics in Europe [1], such collaboration relies on natural interaction between human and robot. It is anticipated that a human-like robot behavior enhances human-robot collaboration.

One basic scenario of human-robot collaboration is that of a human handing over an object to a robot. More specifically, this entails a human hand holding an object while reaching towards a robot to hand over that object to the robot end effector. A handover can be divided into a reaching phase, during which the human hand carries an object towards the handover point, and the phase where control of the object is transferred from the human hand to the robotic hand. In human-human handovers, the agents can anticipate each other's actions to some extend. This allows the receiving agent to already move towards an anticipated handover place while the giving agent reaches for that point.

For a human-robot handover to be done as seamlessly as between humans, the robot has to predict where and when the handover will take place and reach that point with its end effector sufficiently fast to receive the object in a human-like fashion. In this work we perform such a prediction by using prior knowledge on how humans move during a handover.

Our approach uses a dynamic movement primitive as a representation of possible and likely human trajectories and learn it from a demonstration. The parameters of this nonlinear dynamical system describing handover place and time are estimated on-line for handovers similar to the demonstration. The estimation of these parameters then allows the design of an adaptive controller controlling the robot in a human-robot handover.

The paper is structured as follows: In Section II, the state of the art in related work is reviewed. The prediction problem is formulated as a model-based parameter estimation problem in Section III. Subsequently, the predictor is designed and its convergence shown in Section IV. Simulation results based on generated as well as captured data are presented in Section V and conclusions are drawn in Section VI.

II. Related Work

There exists a considerable array of research work in fields related to human-robot collaboration. Human-robot handovers as complex collaborations have been investigated by Strabala *et al.* [2]. They identify two processes that constitute the coordination of two actors handing over an object to one another: A physical process of moving and a cognitive process of exchanging information. In [3], Huber *et al.* focus on the physical process of a robot-human handover by analyzing the importance of human-like motion. Interaction was found to be smoother when the robot was following minimum-jerk trajectories. Work from Flash and Hogan confirms that human point-to-point motions, being an essential part of handovers, exhibit high smoothness originating from their minimum-jerk properties [4]. While the above works focus on the motion involved in handovers, Kim *et al.* consider grasp planning of the robot for handover operations between human and robot [5]. Taking into account constraints like object shapes and functions as well as safety and social constraints, they propose an algorithm coping with different handover scenarios ranging from one-handed to two-handed handovers. Edsinger and Kemp consider experiments with robots and humans handing objects to one another taking a high-level perspective [6]. They show that both the human's as well as the robot's skills complement each other advantageously. While the human solves potentially difficult grasping problems for the robot by directly placing objects into its end effector in a favorable configuration, the robot simplifies the transfer by reaching towards the human.

[1] The authors are with the Division of Systems and Control, Dept. of Electrical Engineering, Chalmers University of Technology, SE-412 96 Gothenburg, Sweden, e-mail: dominik.widmann@live.de; yiannis@chalmers.se

[2] Y. Karayiannidis is also with the Dept. of Robotics, Perception and Learning, School of Electrical Engineering and Computer Science, Royal Institute of Technology (KTH), SE-100 44 Stockholm, Sweden, e-mail: yiankar@kth.se

To control a robot during a handover scenario, human motion has to be considered in the control design. The minimum-jerk properties observed in several papers can be exploited to find a parameterization of human motion. Different approaches to parameterize trajectories exist. Khansari-Zadeh and Billard present a method to learn point-to-point motions from a set of demonstrations. They use a nonlinear autonomous dynamical system to describe a movement and provide sufficient conditions to ensure global asymptotic stability at the endpoint of the movement trajectory [7]. The parameters of the nonlinear system are learned via a so called Stable Estimator of Dynamical Systems (SEDS), thus allowing the dynamical system to be used to program a robot to perform point-to-point motion and to respond to perturbations immediately and appropriately.

While SEDS rely on multiple demonstrations to learn system parameters and parameterize motion, a different concept, only relying on one demonstration, is the dynamic movement primitive (DMP) introduced by Schaal *et al.* [8]. Using a combination of linear and nonlinear autonomous differential equations, a DMP creates smooth motion of a shape that resembles that of a demonstration motion. DMPs with added coupling terms allow for flexible and reactive motion planning and execution, e.g. for robot end effectors. Thanks to the linear parameterization of DMPs and certain invariance properties, DMPs can be learned from one demonstration via supervised learning and can also be used for movement recognition. Ijspeert *et al.* use DMPs to model attractor behaviors of autonomous nonlinear dynamical systems, which makes DMPs a parameterization of trajectories [9], [10]. Instead of a time-dependent function, a trajectory is then described by a dynamical system. Hoffmann *et al.* investigate a biologically inspired modification of the original DMP framework, extending a DMP to let a robot avoid obstacles in a human-like way. They also render this modified DMP more versatile as compared to the original DMP by solving scaling issues of the original DMP. DMPs have been applied by Prada *et al.* to control a robot to perform a human-robot handover by directly feeding a measurement of the human hand position into a DMP as the current goal [11], [12]. The DMP is used as a control law to define a trajectory to a previously unknown handover place. While the simplicity of the DMP-based control law allows for relatively easy realization of their algorithm, the resulting robot trajectories clearly differ from human trajectories due to the constantly changing current position of the human hand that is being used as a goal of the DMP.

A different approach is to estimate unknown high-level parameters of a parameterization of human motion on-line to predict where and when a human-robot handover will take place and control the robot based on this prediction. This leads to the common combination of a parameter estimator and a control law depending on the estimated parameters used in adaptive control.

Parameterizing human motion with a minimum-jerk trajectory and using a discrete-time recursive nonlinear least-squares algorithm for estimation purposes, Maeda *et al.* predict human motion during human-robot handover tasks [13]. While promising results were obtained, their method is restricted to minimum-jerk like movements of the human agent during a handover. In contrast, DMPs pose a parameterization of motion learned from a demonstration trajectory and can thus represent many forms of sufficiently smooth point-to-point motion. To estimate its high-level parameters on-line, a nonlinear estimation algorithm is required.

Extended Kalman filters (EKFs) are often used as nonlinear on-line state or parameter estimators with fast local convergence [14], [15]. Various aspects of industrial application and implementation of the EKF are discussed in [16]. The stability of the EKF has been investigated in numerous publications. Bonnabel and Slotine analyze the contraction properties of the EKF as a nonlinear observer and prove exponential convergence of the state estimation error under some conditions concerning the detectability and nonlinearity of the plant [17]. Ni and Zhang prove stability of the Kalman filter for output error systems [18], which implies no need for artificially introduced process noise in the filter design. Another modification of the EKF allowed Reif *et al.* to improve the speed and the domain of convergence of the estimation error for nonlinear systems with the help of a term of instability added to the classical EKF [19].

We consider the prediction of handover place and time as an on-line parameter estimation problem. The contributions of this paper are:

- In contrast to [13], human motion is parameterized with a DMP allowing for a more versatile algorithm that is applicable to predict duration and endpoint of many different point-to-point trajectories.
- Thanks to the prediction of the handover place and time, the robot end effector can be controlled to move along human-like trajectories towards the predicted handover place and reach it in time for the predicted handover time. This is expected to allow for more seamless human-robot handovers than the approach from [11], [12], where the desired trajectory of the robot end effector was planned to end at the currently measured position of the human hand.
- The presented prediction algorithm is not limited to the specific human-robot handover scenario but can be seen as a general approach to predict goal and timescale of a trajectory having a shape that is similar to an available demonstrated trajectory.

III. Methods

The on-line prediction of place and time of a human-robot handover can be addressed as a model-based on-line parameter estimation problem.

A. Predictor Structure

We can use prior knowledge on human motion to parameterize human motion with a DMP that is learned off-line by demonstration. This DMP has a point attractor at the goal g, representing the handover place, and a certain timescale τ, representing the handover time. Treating these

two parameters as unknown, an EKF-based on-line estimation scheme can be designed to estimate g and τ using available measurements of the human hand position y. Hence, the prediction of handover place and time can be reduced to parameter estimation of the goal and timescale of a DMP. The structure of the resulting predictor, consisting of a DMP parameterizing human motion, and an EKF estimating its parameters on-line based on measurements of the human hand, is illustrated in Figure 1.

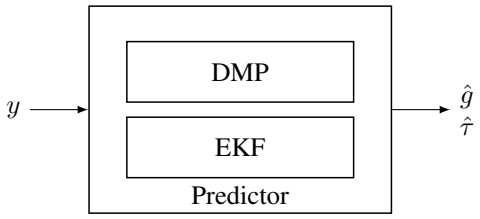

Fig. 1: Overall structure of the proposed predictor.

B. Dynamic Movement Primitives

A DMP is a nonlinear dynamical system with a point attractor that can represent point-to-point trajectories. As presented in [10], it consists of a so called *transformation system*, reading

$$\tau^2 \ddot{y} = \alpha_z(\beta_z(g-y) - \tau\dot{y}) + f(x,g), \tag{1}$$

with initial conditions $y(0) = y_0$, $\dot{y}(0) = y_1$, where α_z, β_z are constants chosen such that (1) is critically damped for $f = 0$. The timescale of (1) is denoted by τ and its point-attractor by the goal g. The phase variable x is produced by the *canonical system*

$$\tau\dot{x} = -\alpha_x x \tag{2}$$

with $\alpha_x > 0$, $x(0) = 1$ and drives the nonlinear forcing term

$$f(x,g) = \frac{\sum_{i=1}^{N} \Psi_i(x) w_i}{\sum_{i=1}^{N} \Psi_i(x)} x(g - y_0), \tag{3}$$

where each of the N exponential basis functions Ψ_i is weighted by a w_i. The basis functions can be chosen as

$$\Psi_i(x) = \exp\left(-h_i(x - c_i)^2\right),$$

with $h_i > 0$ and c_i being constants determining their widths and centers respectively. To allow for good fitting of the DMP to a *training trajectory* obtained from demonstration, the centers of the basis functions Ψ_i are exponentially spaced in x to achieve equal spacing in time [10]. Similarly, the basis functions are set to have equal widths in time.

The dynamical system described by the equations (1) and (2) forms a DMP for one degree of freedom (DOF). Using a known training trajectory $y_{train}(t)$, $\dot{y}_{train}(t)$, $\ddot{y}_{train}(t)$ with known g and τ, the weights w_i of the forcing term can be learned off-line to approximate

$$f_{target} = \tau^2 \ddot{y}_{train} + \tau\alpha_z \dot{y}_{train} - \alpha_z\beta_z(g - y_{train})$$

with (3) as done in [8]. Thanks to its invariance properties [10], a DMP thus constitutes a dynamical system producing trajectories that all have the same shape as the training trajectory, yet can have any nontrivial goal and timescale.

C. The Modified Extended Kalman Filter

To estimate the states of a nonlinear system, a modified EKF presented in [19] can be designed. Consider a nonlinear system

$$\dot{\boldsymbol{x}} = \boldsymbol{f}(\boldsymbol{x}, t), \tag{4}$$

$$\boldsymbol{y} = \boldsymbol{h}(\boldsymbol{x}, t), \tag{5}$$

where $\boldsymbol{x} \in \mathcal{R}^n$ is the state vector, $t \geq t_0 \in \mathcal{R}_{\geq 0}$ denotes time and $\boldsymbol{y} \in \mathcal{R}^p$ represents the measured output and the nonlinear functions $\boldsymbol{f}$ and $\boldsymbol{h}$ are $\mathcal{C}^1$-functions. As presented in [19], an observer for the nonlinear system (4), (5) is given by

$$\dot{\hat{\boldsymbol{x}}} = \boldsymbol{f}(\hat{\boldsymbol{x}}, t) + \boldsymbol{K}(t)(\boldsymbol{y} - \boldsymbol{h}(\hat{\boldsymbol{x}}, t)), \tag{6}$$

with $\hat{\boldsymbol{x}} \in \mathcal{R}^n$ being the estimated state with initial estimate $\hat{\boldsymbol{x}}(0) = \hat{\boldsymbol{x}}_0$ and the time-variant Kalman gain

$$\boldsymbol{K}(t) = \boldsymbol{P}(t)\boldsymbol{C}(\hat{\boldsymbol{x}}, t)^\top \boldsymbol{R}^{-1}, \tag{7}$$

which depends on the solution of the differential Riccati equation

$$\begin{aligned}\dot{\boldsymbol{P}}(t) =& (\boldsymbol{A}(\hat{\boldsymbol{x}}, t) + \alpha\mathbf{I})\boldsymbol{P}(t) + \boldsymbol{P}(t)(\boldsymbol{A}(\hat{\boldsymbol{x}}, t)^\top + \alpha\mathbf{I}) + \boldsymbol{Q} \\ &- \boldsymbol{P}(t)\boldsymbol{C}(\hat{\boldsymbol{x}}, t)^\top \boldsymbol{R}^{-1}\boldsymbol{C}(\hat{\boldsymbol{x}}, t)\boldsymbol{P}(t),\end{aligned} \tag{8}$$

with $\boldsymbol{P}(0) = \boldsymbol{P}_0$, α being a positive constant, $\boldsymbol{Q}$ and $\boldsymbol{R}$ being constant positive definite matrices. Note that (8) is a differential Riccati equation modified in [19] by introducing $\alpha > 0$ that denotes the degree of stability. The matrices $\boldsymbol{A}(\hat{\boldsymbol{x}}, t)$ and $\boldsymbol{C}(\hat{\boldsymbol{x}}, t)$ are obtained using the linearizations

$$\boldsymbol{A}(\hat{\boldsymbol{x}}, t) = \left.\frac{\partial \boldsymbol{f}}{\partial \boldsymbol{x}}(\boldsymbol{x}, t)\right|_{\boldsymbol{x}=\hat{\boldsymbol{x}}}, \tag{9}$$

$$\boldsymbol{C}(\hat{\boldsymbol{x}}, t) = \left.\frac{\partial \boldsymbol{h}}{\partial \boldsymbol{x}}(\boldsymbol{x}, t)\right|_{\boldsymbol{x}=\hat{\boldsymbol{x}}}. \tag{10}$$

Note that via (9) and (10), the nonlinearities (4) and (5) can be extended into the power series

$$\boldsymbol{f}(\boldsymbol{x}, t) - \boldsymbol{f}(\hat{\boldsymbol{x}}, t) = \boldsymbol{A}(\hat{\boldsymbol{x}}, t)(\boldsymbol{x} - \hat{\boldsymbol{x}}) + \boldsymbol{\Phi}(\boldsymbol{x}, \hat{\boldsymbol{x}}), \tag{11}$$

$$\boldsymbol{h}(\boldsymbol{x}, t) - \boldsymbol{h}(\hat{\boldsymbol{x}}, t) = \boldsymbol{C}(\hat{\boldsymbol{x}}, t)(\boldsymbol{x} - \hat{\boldsymbol{x}}) + \boldsymbol{\Psi}(\boldsymbol{x}, \hat{\boldsymbol{x}}), \tag{12}$$

where $\boldsymbol{\Phi}$ and $\boldsymbol{\Psi}$ are the terms of second and higher order. To ensure local convergence of the modified EKF, the following assumptions from [19] have to hold:

Assumption 1. *There exist* $\underline{p}_c, \overline{p}_c > 0$ *such that*

$$\underline{p}_c \mathbf{I} \leq \boldsymbol{P}(t) \leq \overline{p}_c \mathbf{I}, \ \forall t \in \mathcal{R}_{\geq 0}.$$

Assumption 2. *There exist* $\kappa_\Phi, \kappa_\Psi, \epsilon_\Phi, \epsilon_\Psi > 0$*, such that the nonlinearities* $\boldsymbol{\Phi}$*,* $\boldsymbol{\Psi}$*, given by* (11) *and* (12) *are bounded as follows:*

$$\|\boldsymbol{\Phi}(\boldsymbol{x}, \hat{\boldsymbol{x}})\| \leq \kappa_\Phi \|\boldsymbol{x} - \hat{\boldsymbol{x}}\|^2, \tag{13}$$

$$\|\boldsymbol{\Psi}(\boldsymbol{x}, \hat{\boldsymbol{x}})\| \leq \kappa_\Psi \|\boldsymbol{x} - \hat{\boldsymbol{x}}\|^2, \tag{14}$$

for $\|\boldsymbol{x} - \hat{\boldsymbol{x}}\| \leq \epsilon_\Phi$, $\|\boldsymbol{x} - \hat{\boldsymbol{x}}\| \leq \epsilon_\Psi$ *respectively.*

Assumption 3. *The time-varying matrix $\boldsymbol{C}(\hat{\boldsymbol{x}}, t)$ from* (10) *is bounded as follows:*

$$\|\boldsymbol{C}(\hat{\boldsymbol{x}}, t)\| \leq \bar{c},$$

for all $t \geq t_0$ for a $\bar{c} \in \mathcal{R}_{>0}$.

Under Assumptions 1, 2 and 3, the observer given by (6), (7) and the Riccati equation (8) is an exponential observer for the nonlinear system (4), (5) and the estimation error $\boldsymbol{\xi} = \boldsymbol{x} - \hat{\boldsymbol{x}}$ decays exponentially to zero with a time constant $\tau_\xi > \alpha$, [19].

IV. Predictor Design

A. Modified EKF-Based State Estimation for one DOF

The estimation of the parameters of a DMP can be put into a state estimation context by simply including the unknown parameters in the state vector of an observer.

1) Observer Formulation: To estimate the unknown goal g and timescale τ of the nonlinear DMP (1), (2), we introduce the state vector

$$\boldsymbol{x} = \begin{bmatrix} x & y & z & g & \tau \end{bmatrix}^\top. \tag{15}$$

Note that, in a handover context, the inclusion of both position y and velocity z of the humand hand in the state vector $\boldsymbol{x}$ means that we estimate the state of the human hand, also commonly referred to as tracking, as well as the handover place g and time τ. Depending on the available measurements, different choices of $\boldsymbol{x}$ are possible. In case all states of the human hand are measurable, pure prediction of the handover by means of an EKF with states g and τ is possible.

Given the state vector (15) the nonlinear system consisting of the DMP dynamics and the parameter dynamics is written as follows:

$$\begin{aligned} \dot{\boldsymbol{x}} &= \boldsymbol{f}(\boldsymbol{x}) \\ &= \begin{bmatrix} -\frac{\alpha_x}{\tau} x \\ z \\ \alpha_z \left(\frac{\beta_z}{\tau^2}(g - y) - \frac{z}{\tau} \right) + \frac{f(x,g)}{\tau^2} \\ 0 \\ 0 \end{bmatrix}. \end{aligned}$$

Assuming the position y is measurable, we obtain the linear measurement model

$$y = h(\boldsymbol{x}) = \boldsymbol{C}\boldsymbol{x}, \tag{16}$$

with

$$\boldsymbol{C} = \begin{bmatrix} 0 & 1 & 0 & 0 & 0 \end{bmatrix}. \tag{17}$$

Note that additional measurements can easily be included by appropriately changing matrix $\boldsymbol{C}$. In order to use the modified EKF to estimate the state vector (15), using the initial conditions of the DMP, the initial estimate of the EKF can be set to $\hat{\boldsymbol{x}}(0) = [1, y_0, y_1, \hat{g}_0, \hat{\tau}_0]^\top$ where $\hat{g}_0$ and $\hat{\tau}_0$ are initial estimates for goal g and timescale τ. The initial position can be chosen as $y_0 = 0$ without loss of generality since any trajectory can be shifted to start at zero by a simple coordinate transformation. The linearization from (9) evaluates to

$$\begin{aligned} \boldsymbol{A}(\hat{\boldsymbol{x}}) &= \left. \frac{\partial \boldsymbol{f}(\boldsymbol{x})}{\partial \boldsymbol{x}} \right|_{\boldsymbol{x}=\hat{\boldsymbol{x}}} \\ &= \left. \begin{bmatrix} -\frac{\alpha_x}{\tau} & 0 & 0 & 0 & \frac{\alpha_x}{\tau^2} x \\ 0 & 0 & 1 & 0 & 0 \\ \frac{1}{\tau^2} \frac{\partial f(x,g)}{\partial x} & -\frac{\alpha_z \beta_z}{\tau^2} & -\frac{\alpha_z}{\tau} & A_{34} & A_{35} \\ 0 & 0 & 0 & 0 & 0 \\ 0 & 0 & 0 & 0 & 0 \end{bmatrix} \right|_{\boldsymbol{x}=\hat{\boldsymbol{x}}}, \end{aligned} \tag{18}$$

with

$$\begin{aligned} A_{34} &= \frac{1}{\tau^2} \left(\alpha_z \beta_z + \frac{\partial f(x,g)}{\partial g} \right), \\ A_{35} &= \frac{\alpha_z z}{\tau^2} - \frac{2}{\tau^3} \left(\alpha_z \beta_z (g - y) + f(x,g) \right), \end{aligned}$$

where

$$\frac{\partial f}{\partial g}(x,g) = \tilde{f}(x) = \frac{\sum_{i=1}^N \Psi_i(x) w_i}{\sum_{i=1}^N \Psi_i(x)} x.$$

Furthermore, it is

$$\frac{\partial f}{\partial x}(x,g) = g \tilde{f}'(x), \tag{19}$$

with

$$\begin{aligned} \tilde{f}'(x) =& \frac{\sum_{i=1}^N \Psi_i(x) w_i}{\sum_{i=1}^N \Psi_i(x)} + x \frac{\left(\sum_{i=1}^N \Psi_i'(x) w_i \right)}{\sum_{i=1}^N \Psi_i(x)} \\ & - x \frac{\left(\sum_{i=1}^N \Psi_i(x) w_i \right) \left(\sum_{i=1}^N \Psi_i'(x) \right)}{\left(\sum_{i=1}^N \Psi_i(x) \right)^2}, \end{aligned}$$

and

$$\Psi_i'(x) = -2 h_i (x - c_i) \Psi_i(x).$$

Consequently, an estimator for the states of the DMP and its unknown timescale and goal is given by the modified EKF (6), (7) and (8) with matrices $\boldsymbol{C}$ and $\boldsymbol{A}(\hat{\boldsymbol{x}})$ given by (17) and (18) respectively.

2) Stability: For sufficiently varying trajectories $y(t)$ and sufficiently good state estimates $\hat{\boldsymbol{x}}(t)$ for $t \in [0, T]$ with $T \geq \tau$, detectability of $\boldsymbol{A}(\hat{\boldsymbol{x}})$, $\boldsymbol{C}$ can be ensured up to time T via positive definite lower and upper bounds to the corresponding observability grammian [20]. Consequently, Assumption 1 holds up to time T [17].

As the measurement model (16) is linear, (14) holds for all $\epsilon_\Psi > 0$ with $\|\boldsymbol{x} - \hat{\boldsymbol{x}}\| \leq \epsilon_\Psi$. Therefore, for Assumption 2 to hold, it remains to show that the nonlinearity

$$\boldsymbol{\Phi}(\boldsymbol{x}, \hat{\boldsymbol{x}}) = \boldsymbol{f}(\boldsymbol{x}) - \boldsymbol{f}(\hat{\boldsymbol{x}}) - \boldsymbol{A}(\hat{\boldsymbol{x}})(\boldsymbol{x} - \hat{\boldsymbol{x}}),$$

satisfies (13) for some $\epsilon_\Phi > 0$ and $\|\boldsymbol{x} - \hat{\boldsymbol{x}}\| \leq \epsilon_\Phi$. To show this, we first establish that $\partial \boldsymbol{f} / \partial \boldsymbol{x}$ is locally Lipschitz: Clearly, all linear terms in (18) are Lipschitz. It remains to check the appearing nonlinear terms f, $\partial f / \partial x$ and $\partial f / \partial g$ for local Lipschitz continuity. To check Lipschitz continuity of $\partial f / \partial x$, using (19), we calculate $\partial / \partial \boldsymbol{x} \, (\partial f / \partial x) =$

TABLE I: DMP parameters

Parameter	Value
α_z	25
β_z	$\alpha_z/4$
α_x	$\alpha_z/3$
N	30

$[g\tilde{f}'', 0, 0, \tilde{f}', 0]$. Considering the fact that the basis functions Ψ_i are Gaussians and that the weights w_i are bounded by construction, local boundedness of $\tilde{f}'$ and $\tilde{f}''$ can be shown for a sufficiently large number of basis functions N as well as basis function parameters h_i and c_i that ensure overlap between the basis functions. Consequently, for any finite goal g, $\partial f/\partial x$ is locally Lipschitz which also implies that f is locally Lipschitz. Similarly, thanks to the local boundedness of $\tilde{f}'$, $\partial f/\partial g$ is locally Lipschitz as well and hence we can conclude that $\partial \boldsymbol{f}/\partial \boldsymbol{x}$ is locally Lipschitz. Thus, using the monotony of the integral, $\|\boldsymbol{\Phi}(\boldsymbol{x}, \hat{\boldsymbol{x}})\| \leq \kappa_A \|\boldsymbol{x} - \hat{\boldsymbol{x}}\|^2$ holds for some $\epsilon_\Phi > 0$ with $\|\boldsymbol{x} - \hat{\boldsymbol{x}}\| \leq \epsilon_\Phi$ and consequently Assumption 2 is satisfied.

Furthermore, thanks to the linearity of the measurement model (16), Assumption 3 holds as well and local convergence of the modified EKF designed based on a DMP is ensured.

B. Extension to Multiple DOF

As suggested by [10], the one-dimensional DMP can be supplemented with $n-1$ additional transformation systems (1) to represent motion in n dimensions. Since the trajectories of an object in the different dimensions are temporarily coupled, the transformation systems can share one canonical system (2). This results in the state vector $\boldsymbol{x} = [x, y_1, \dot{y}_1, \ldots, y_n, \dot{y}_n, g_1, \ldots, g_n, \tau]^\top \in \mathcal{R}^{2+3n}$ containing the phase variable x, the states of the transformation systems y_j, $\dot{y}_j$ with $j = 1, \ldots, n$, their goals g_j and the shared timescale τ.

For measurable positions y_j, this results into an improving relation between the number of states and the number of measurable system outputs for $n > 1$. Assumptions 1, 2 and 3 can be shown to hold in the n-dimensional case using similar arguments as in the one-dimensional case above.

V. Results

Conducting simulations, we first validate the presented approach for generated one-dimensional trajectories. Subsequently, the predictor is extended and used to predict two-dimensional motion, such as motion in a plane. Finally, real data is used to evaluate the robustness of the predictor to modeling errors.

A. Proof of Concept

We first use the one-dimensional minimum-jerk training trajectory from Figure 2 with starting point $y_0 = 0\,\mathrm{m}$, endpoint $g = 2\,\mathrm{m}$ and transition time $\tau = 10\,\mathrm{s}$ to learn a DMP with the parameters from Table I representing human motion in one dimension. The remaining trajectories are used as test trajectories to validate that the predictor works for different goals and timescales. The modified EKF is implemented using the tuning parameters from Table II. Figure 3 and Figure 4 show the estimation errors $\tilde{g} = g - \hat{g}$ and $\tilde{\tau} = \tau - \hat{\tau}$ for goal and timescale of the DMP respectively. Goal and timescale of all the trajectories from Figure 2 are predicted with the parameters of the training trajectory $\hat{g}_0 = 2\,\mathrm{m}$ and $\hat{\tau}_0 = 4\,\mathrm{s}$ as initial guesses.

TABLE II: Parameters of the modified EKF

Parameter	Value
$\boldsymbol{P}_0$	$10^4 \boldsymbol{I}$
$\boldsymbol{R}$	$\boldsymbol{I}$
$\boldsymbol{Q}$	$\mathrm{diag}(0.1, 0.1, 0.1, 10^4, 10^4)$
α	2

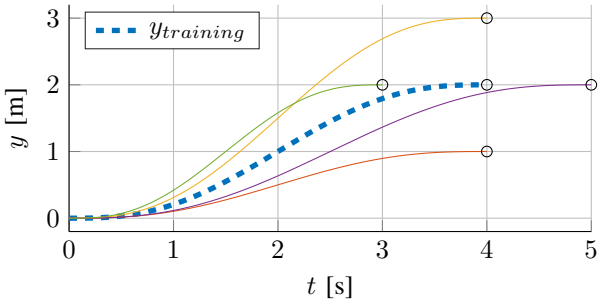

Fig. 2: Minimum-jerk trajectories with different goals and timescales.

We observe that most of the goal estimation errors in Figure 3 are close to zero after about 0.6τ while the timescale estimation errors in Figure 4 tend to zero more slowly. The goal estimation works well for all the trajectories and thus allows for good prediction of the handover place in the one-dimensional case.

B. Two-Dimensional Case

To validate that the prediction works for two-dimensional motion, the proposed predictor is used on the trajectories from Figure 5. Figure 6 depicts the resulting parameter estimation errors $\tilde{g}_j = g_j - \hat{g}_j$ with $j = 1, 2$ and $\tilde{\tau}$ when using a DMP with parameters from Table I and a modified EKF with parameters from Table III as part of a 2d-predictor jointly predicting goal and timescale of $y_1(t)$ and $y_2(t)$. It also shows the parameter estimation errors obtained by

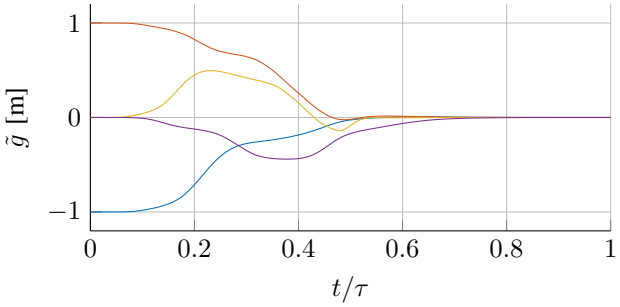

Fig. 3: Goal estimation errors $\tilde{g}$ for minimum-jerk trajectories using initial guesses $\hat{g}_0 = 2\,\mathrm{m}$ and $\hat{\tau}_0 = 4\,\mathrm{s}$.

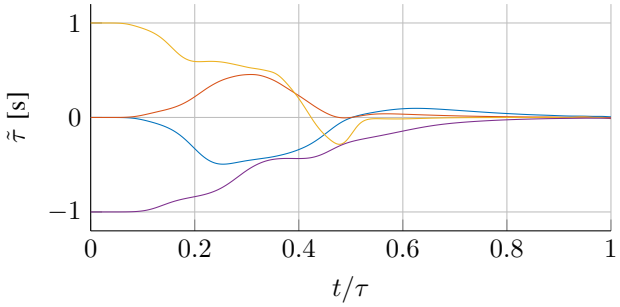

Fig. 4: Timescale estimation errors $\tilde{\tau}$ for minimum-jerk trajectories using initial guesses $\hat{g}_0 = 2\,\mathrm{m}$ and $\hat{\tau}_0 = 4\,\mathrm{s}$.

TABLE III: Parameters of the modified EKF in the 2d-case.

Parameter	Value
$\boldsymbol{P}_0$	$10^4\boldsymbol{I}$
$\boldsymbol{R}$	$\boldsymbol{I}$
$\boldsymbol{Q}$	$\mathrm{diag}(0.1, 0.1, 0.1, 0.1, 0.1, 10^4, 10^4, 10^4)$
α	2

using separate 1d-predictors on $y_1(t)$ and $y_2(t)$. Clearly, the 2d-predictor exhibits faster convergence of the parameter estimates by exploiting the fact that both trajectories have a shared timescale. The 1d-predictor is slower to estimate g_1 and therefore it takes longer to obtain a good prediction of the handover place. We can conclude that convergence of a 2d-predictor can benefit from a highly excited trajectory in one dimension making it more effective than using two 1d-predictors.

C. Real Data: Robustness to Modeling Errors

The robustness to modeling errors of the proposed predictor is evaluated with the trajectories captured during real human-human handovers [1] depicted in Figure 7. The labeled training trajectory is used to learn a DMP with parameters from Table I except for an increased number $N = 100$ of basis functions to ensure good fitting to the more complex trajectories. This learned DMP is an erroneous model for the remaining trajectories as they do not have the same shape as the training trajectory.

Using the EKF parameters from Table IV as well as initial guesses $\hat{g}_0 = -1\,\mathrm{m}$ and $\hat{\tau}_0 = 3\,\mathrm{s}$, the estimation errors for the goals and timescales are shown in Figure 8 and Figure 9 respectively.

While in Figure 8 the goal estimates are close to the true goals after around 0.7τ for all captured trajectories, the timescale estimates from Figure 9 are only close to the true timescale for the training trajectory. We conclude that the modeling errors mainly cause erroneous timescale estimates. The goal estimates, however, are reliable despite the modeling errors, implying that the prediction of handover places shows robustness to modeling errors and can thus also be used for trajectories with a slightly different shape as compared to the training trajectory.

[1] The handover trajectories were captured by Axel Demborg and Elon Såndberg in a motion capture lab at KTH as part of their Bachelor's thesis.

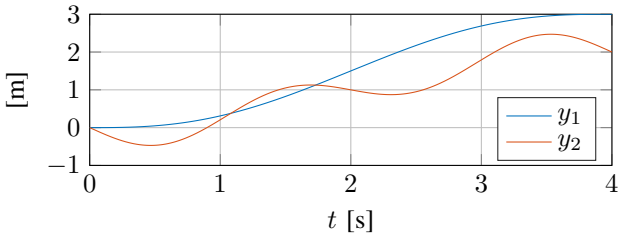

Fig. 5: Complex two-dimensional trajectory.

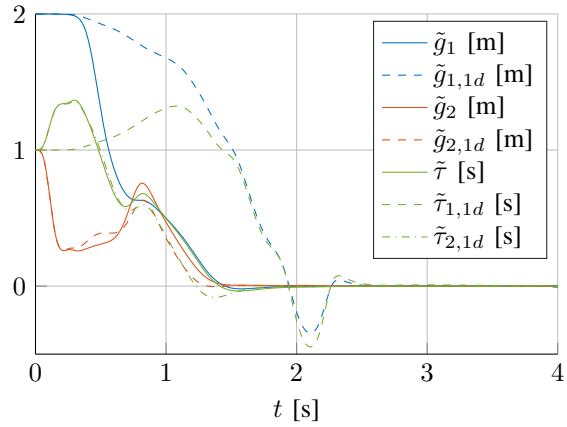

Fig. 6: Comparison of parameter estimation errors for a complex 2d-trajectory using a 2d-predictor (solid lines, $\tilde{g}_1$, $\tilde{g}_2$, $\tilde{\tau}$) and two 1d-predictors (dashed lines, $\tilde{g}_{1,1d}$, $\tilde{\tau}_{1,1d}$ and $\tilde{g}_{2,1d}$, $\tilde{\tau}_{2,1d}$) with true parameters $g_1 = 3\,\mathrm{m}$, $g_2 = 2\,\mathrm{m}$ and $\tau = 4\,\mathrm{s}$ and initial guesses $\hat{g}_{1,0} = \hat{g}_{2,0} = 1\,\mathrm{m}$ and $\hat{\tau}_0 = 3\,\mathrm{s}$.

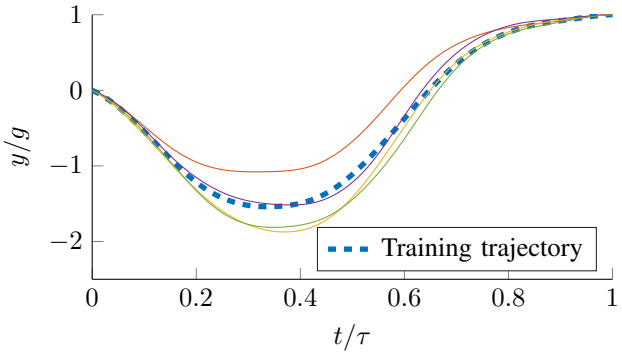

Fig. 7: Captured trajectories involved in human-human handovers.

TABLE IV: Parameters of the modified EKF for real data.

Parameter	Value
$\boldsymbol{P}_0$	$10^4\boldsymbol{I}$
$\boldsymbol{R}$	$0.001\boldsymbol{I}$
$\boldsymbol{Q}$	$\mathrm{diag}(0.1, 0.1, 0.1, 0.1, 0.1, 10^4, 10^4, 10^4)$
α	5

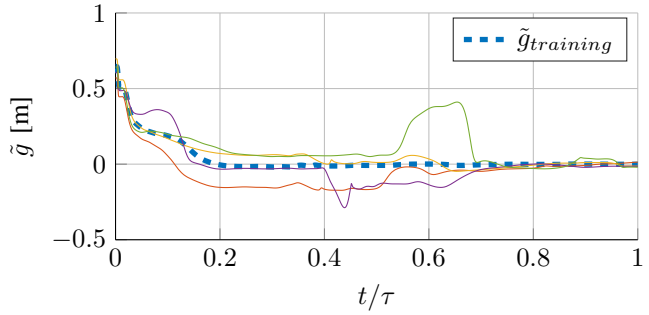

Fig. 8: Goal estimation errors for captured human-human handovers using initial guesses $\hat{g}_0 = \hat{g}_{2,0} = -1\,\mathrm{m}$ and $\hat{\tau}_0 = 3\,\mathrm{s}$.

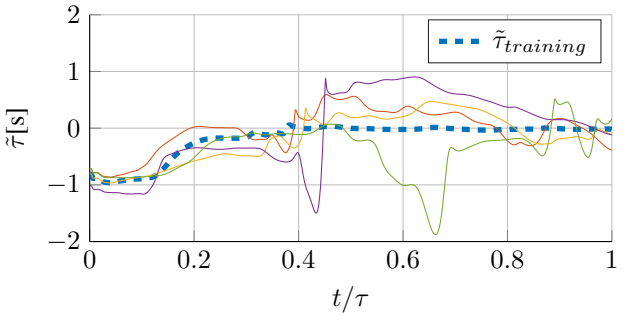

Fig. 9: Goal estimation errors for captured human-human handovers using initial guesses $\hat{g}_0 = \hat{g}_{2,0} = -1\,\mathrm{m}$ and $\hat{\tau}_0 = 3\,\mathrm{s}$.

VI. Conclusions

A predictor performing on-line estimation of goal and timescale of a dynamic movement primitive (DMP) with a modified extended Kalman filter has been presented. After learning a DMP from a sufficiently smooth point-to-point training trajectory, goals and timescales of similar trajectories could be predicted on-line provided they were sufficiently excited. The predictor was applied to human-robot handovers and was able to predict place and time of a handover on-line while only measuring the position of the human hand. Robustness to modeling errors allowed for prediction of the handover place despite different shapes of training and testing trajectories.

As a next step, an adaptive controller using the predictions provided by the proposed predictor can be designed to adaptively control a robot and achieve more seamless human-robot handovers.

The available estimates of timescale and point attractor of a nonlinear system allow for applications of the proposed algorithm to interesting problems that go beyond the prediction of handovers. Further applications could be the prediction of motion in general or the synchronization of multi-agent systems.

Acknowledgment

We would like to thank Christian Smith, Axel Demborg and Elon Såndberg from KTH for providing us with useful experimental data on human-human handovers.

References

[1] B. Liepert *et al.*, "Strategic research agenda for robotics in europe," Technical report, The European Robotics Technology Platform (EUROP), Tech. Rep., 2009.

[2] K. W. Strabala, M. K. Lee, A. D. Dragan, J. L. Forlizzi, S. Srinivasa, M. Cakmak, and V. Micelli, "Towards seamless human-robot handovers," *Journal of Human-Robot Interaction*, vol. 2, no. 1, pp. 112–132, 2013.

[3] M. Huber, M. Rickert, A. Knoll, T. Brandt, and S. Glasauer, "Human-robot interaction in handing-over tasks," in *RO-MAN 2008 - The 17th IEEE International Symposium on Robot and Human Interactive Communication*, Aug 2008, pp. 107–112.

[4] T. Flash and N. Hogan, "The coordination of arm movements: an experimentally confirmed mathematical model," *The journal of Neuroscience*, vol. 5, no. 7, pp. 1688–1703, 1985.

[5] J. Kim, J. Park, Y. K. Hwang, and M. Lee, "Advanced grasp planning for handover operation between human and robot," in *2nd International Conference on Autonomous Robots and Agents*, 2004, pp. 13–15.

[6] A. Edsinger and C. C. Kemp, "Human-robot interaction for cooperative manipulation: Handing objects to one another," in *RO-MAN 2007 - The 16th IEEE International Symposium on Robot and Human Interactive Communication*, Aug 2007, pp. 1167–1172.

[7] S. M. Khansari-Zadeh and A. Billard, "Learning stable nonlinear dynamical systems with gaussian mixture models," *IEEE Transactions on Robotics*, vol. 27, no. 5, pp. 943–957, Oct 2011.

[8] S. Schaal, J. Peters, J. Nakanishi, and A. Ijspeert, "Learning movement primitives," in *Robotics Research. The Eleventh International Symposium*. Springer, 2005, pp. 561–572.

[9] A. J. Ijspeert, J. Nakanishi, and S. Schaal, "Learning attractor landscapes for learning motor primitives," Tech. Rep., 2002.

[10] A. J. Ijspeert, J. Nakanishi, H. Hoffmann, P. Pastor, and S. Schaal, "Dynamical movement primitives: learning attractor models for motor behaviors," *Neural computation*, vol. 25, no. 2, pp. 328–373, 2013.

[11] M. Prada and A. Remazeilles, "Dynamic movement primitives for human robot interaction," in *IEEE/RSJ Int. Conf. on Intelligent Robots and Systems, workshop on Robot Motion Planning: online, reactive and in Real-time, Algarve, Portugal*, 2012.

[12] M. Prada, A. Remazeilles, A. Koene, and S. Endo, "Implementation and experimental validation of dynamic movement primitives for object handover," in *2014 IEEE/RSJ International Conference on Intelligent Robots and Systems*, Sept 2014, pp. 2146–2153.

[13] Y. Maeda, T. Hara, and T. Arai, "Human-robot cooperative manipulation with motion estimation," in *Proceedings of the IEEE/RSJ International Conference on Intelligent Robots and Systems*, vol. 4, 2001, pp. 2240–2245 vol.4.

[14] G. Besançon, *Nonlinear observers and applications*. Springer, 2007, vol. 363.

[15] R. M. Murray, "Optimization-based control," *California Institute of Technology, CA*, 2009.

[16] F. Auger, M. Hilairet, J. M. Guerrero, E. Monmasson, T. Orlowska-Kowalska, and S. Katsura, "Industrial applications of the kalman filter: A review," *IEEE Transactions on Industrial Electronics*, vol. 60, no. 12, pp. 5458–5471, 2013.

[17] S. Bonnabel and J. J. Slotine, "A contraction theory-based analysis of the stability of the deterministic extended kalman filter," *IEEE Transactions on Automatic Control*, vol. 60, no. 2, pp. 565–569, Feb 2015.

[18] B. Ni and Q. Zhang, "Stability of the kalman filter for output error systems," *IFAC-PapersOnLine*, vol. 48, no. 28, pp. 1106–1111, 2015.

[19] K. Reif, F. Sonnemann, and R. Unbehauen, "An EKF-based nonlinear observer with a prescribed degree of stability," *Automatica*, vol. 34, no. 9, pp. 1119–1123, 1998.

[20] P. A. Ioannou and J. Sun, *Robust adaptive control*. Dover Publications, Inc., 2012.